Monolayer Structures of Highly Photoluminescent Furan Oligoaryls: An Approach to Improve Packing Crystallinity of Dithiolated Aromatics

Shu-Yi Lin,[†] I−Wen Peter Chen,[†] Chun-hsien Chen,*[,†] Chin-Fa Lee,[‡] Chih-Ming Chou,[‡] and Tien-Yau Luh*[,‡]

Department of Chemistry, National Tsing Hua University, Hsinchu, Taiwan 30013, Department of Chemistry, National Taiwan University, Taipei, Taiwan 106

Received: December 9, 2004; In Final Form: February 24, 2005

We demonstrated that mono- and dithiolated furan-containing oligoaryls (**II**−**IV**, see Chart 2) can be successfully synthesized via a one-pot strategy starting from propargylic dithioacetals. IRAS (infrared reflection−absorption spectroscopy) and STM (scanning tunneling microscopy) experiments revealed that single-component monolayers of **II**, **III**, and **IV** are essentially disordered, an important property that prevents excited photoluminescent molecules from self-quenching in the organic layers of an OLED device. Surprisingly, localized lattice packing of crystalline dithiolated furan oligoaryls on Au(111) can be assembled by immersing preadsorbed *n*-dodecanethiol SAMs in the corresponding deposition solutions. The discrepancy in the formation of disordered or localized crystalline structures is discussed. For single-component monolayers, the facile formation of S−Au bonds generates chaotically distributed monolayers in which the arched molecules hinge each other and block the desorptive pathways. The absence of crystalline packing is mainly attributed to the difficulty for the dithiols to simultaneously break two S−Au bonds, to desorb, and then to readsorb, the key step to improve the intermolecular attractions for crystalline SAMs. By preassembling *n*-dodecanethiol SAMs, the space for dithiolated compounds **III** and **IV** to adsorb is limited to domain boundaries or packing defects where crystalline packing of **III** and **IV** can grow.

Introduction

Conjugated oligomers with tailored constituents and precisely controllable length have been a current research interest because of their potential applications in molecular wires and optoelectronics.[1,2] The electric and optoelectronic properties of conjugated oligoaryls can occasionally be fine-tuned by integrating with heteroaromatic rings (e.g., oligothiophenes,[2−8] tetrathiafulvalene,[9−12] or pyrroles[1−4,13,14]). Furan-containing oligoaryls,[7,8,15−18] representing a new class of materials, are relatively unexplored. We recently developed a new annulation procedure for the synthesis of 2,3,5-trisubstituted furans from the corresponding propargylic dithioacetals.[19−22] This protocol can conveniently introduce at C_3 position in the furan ring an alkyl substituent, which increases the solubility in organic solvents and thus improve the processibility of these materials.[19−22] It has recently been shown that **I** (**Chart 1**) exhibited excellent hole-transport properties with low turn-on voltage, high efficiency, high brightness, and high hole mobility, comparable with those of conventional arylamine-based hole-transport materials.[23,24] The Bassler formalism,[25−30] referred as a disorder model, was utilized to fit the measured mobility, and the results of data analysis indicated that the layer containing **I** prepared in the OLED device was essentially disordered, presumably resulting from the steric influence and nonplanar structure.[19,23] Such steric hindrance and thus disorderness are favorable in conserving excited fluorophores from self-quenching because of film crystallization.

CHART 1: Structure of Furan, 2,2′-[1,1′-biphenyl]-4,4′-diylbis[3,5-diphenyl-

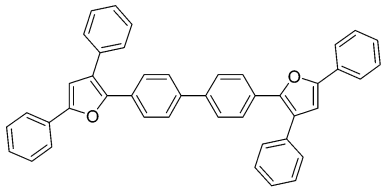

I

Over the past decade, the concept of engineering thioaromatic self-assembled monolayers (SAMs)[31−46] as the building blocks for molecular electronics[45,47−55] has stimulated enormous research activities. There are two general findings for structural characterization of X−$(C_6H_4)_m$−SH SAMs on gold. First, the sulfur headgroup preferentially adopts the sp^3 binding scheme on gold substrate.[35,56−58] For thiolphenol (Ph−SH) and biphenylthiol, the tilt angle of the phenyl introduces steric hindrance between neighboring molecules and, therefore, their SAMs are ill-defined.[34−37,58−64] By inserting a methylene unit between the phenyl ring and the thiol group (i.e., Ph−CH_2−SH), the steric constraint is released and the SAMs become well-ordered.[35,56−58,65] Second, for those not containing a benzyl moiety, increasing intermolecular $\pi-\pi$ interactions by increasing the number of phenyl rings improves the film crystallinity.[34−38,66] In this IRAS (infrared reflection−absorption spectroscopy) and STM (scanning tunneling microscopy) study, we examined the SAM structures of planar furan-containing oligoaryls (**II**−**IV** shown in Chart 2), analogues of **I** that appear disordered as a hole-transport layer in an OLED device (vide supra). Given that the conjugated and planar aryls favorable to the strong neighboring $\pi-\pi$ stacking, the benzyl group adaptable with the sp^3

* Authors to whom correspondence should be addressed. E-mail: chhchen@mx.nthu.edu.tw (C.-h.C.), tyluh@ntu.edu.tw (T.-Y.L.). Phone: +886 3 573 7009 (C.-h.C.), +886 2 2363 6288 (T.-Y.L.). Fax: +886 3 571 1082 (C.-h.C.), +886 2 2364 4971 (T.-Y.L.).

[†] National Tsing Hua University.

[‡] National Taiwan University.

10.1021/jp044404f CCC: $30.25
Published on Web 03/31/2005

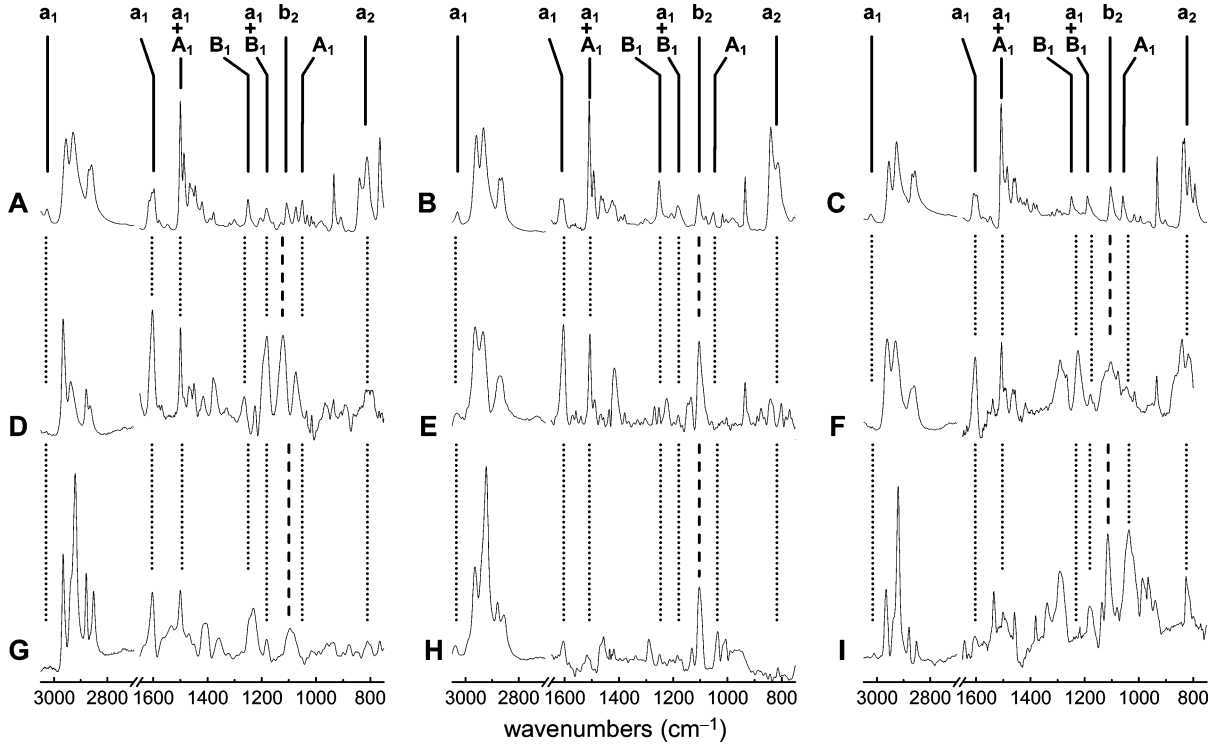

Figure 1. Transmission and IRAS spectra of compounds **II**−**IV**. Samples prepared in KBr pellets: (A) **II**, (B) **III**, and (C) **IV**. Transmittance is converted into absorbance for better comparison with IRAS spectra. Spectra of single-component films: (D) **II**, (E) **III**, and (F) **IV**. Mixed monolayer spectra of (G) **II**, (H) **III**, and (I) **IV**-containing films prepared in *n*-dodecanethiol preassembled gold substrate. The assignments of vibrational modes are tabulated in Table 1.

CHART 2: Structures of Thiolated Furan-containing Oligoaryls

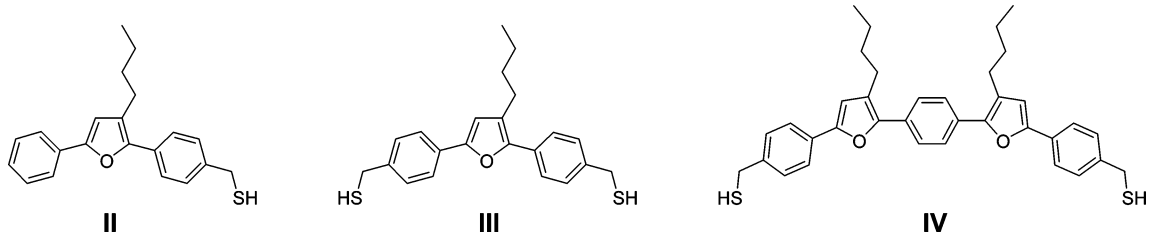

hybridization of S−Au bond, and *n*-butyl side chains that introduce steric effects, it is interesting to find out which factor dominates and whether such furan-containing oligoaryl monolayers are crystalline or disordered, a crucial factor for the organic layer of OLED devices. Also explored is improvement in the packing structure of such branched mercaptoaryls, an important subject in monolayer assembly.

Results

IRAS measurements. Typical IR spectra of **II**, **III**, and **IV** prepared in KBr pellets are shown in panels A, B, and C of Figure 1, respectively. The molecules in KBr pellets are grinded thoroughly and thus are presumably oriented isotropically. The characteristic vibrational peaks for furan ($\mathbf{A_1}$ and $\mathbf{B_1}$)[67,68] and the disubstituted *para*-benzene moiety ($\mathbf{a_1}$, $\mathbf{a_2}$, and $\mathbf{b_2}$)[69−71] are denoted. The bands at 2965−2850 cm^{-1} are the stretch modes for *n*-butyl (ν_{CH2} and ν_{CH3}).[72−76] Summarized in Table 1 are the peak positions and the vibrational modes assigned according to literature reports of similar moieties.[67−76] The band at ∼1504 cm^{-1} is the result of overlap of an $\mathbf{A_1}$ mode of furan moiety[67] with an $\mathbf{a_1}$ of phenyl.[69] Because the two vibrational modes are somewhat perpendicular to each other, these bands are not used to discuss the molecular orientation.

Panels D, E, and F in Figure 1 are, respectively, IRAS spectra of the single-component monolayers on gold for **II**, **III**, and **IV**. The ν(SH) mode is indiscernible, suggesting the formation of a S−Au bond. For the convenience of the following discussion, the transition dipoles[69,77] of the *para*-benzene moiety relative to the surface normal are sketched in Figure 2 in which $\mathbf{a_1}$ (ca. 3052 and 1604 cm^{-1}) and $\mathbf{b_2}$ (∼1106 cm^{-1}) are in-plane vibrational modes and are, respectively, parallel and perpendicular to the C_{2v} axis of this group; $\mathbf{a_2}$ (∼833 cm^{-1}) is an out-of-plane mode. For the furan moiety, the in-plane bending modes $\mathbf{A_1}$ and $\mathbf{B_1}$ are parallel and perpendicular to the C_{2v} axis, respectively. The relative peak intensities of Figure 1D−F are quite different than those of the corresponding spectra measured in KBr pellets (Figure 1A−C). The intensity ratios of $I_{\mathbf{b2}}/I_{\mathbf{a1}\text{ at }3052\text{ cm}^{-1}}$, $I_{\mathbf{b2}}/I_{\mathbf{a2}}$, and $I_{\mathbf{b2}}/I_{\mathbf{a1}+\mathbf{B1}\text{ at }1180\text{ cm}^{-1}}$ increase significantly. Because the peak intensities obtained from KBr pellets represent transition dipoles oriented isotropically and because IRAS for metallic substrates is insensitive to transition dipole perpendicular to the surface normal,[78,79] the increase in these intensity ratios suggests a plausible structure proposed in Figure 2A in which the long axes of the benzene rings (i.e., $\mathbf{a_1}$) are somewhat perpendicular to the surface normal. For the other $\mathbf{a_1}$ at 1603 cm^{-1}, however, the magnitude of $I_{\mathbf{b2}}/I_{\mathbf{a1}}$ ratios of the single component film compared to the corresponding compound in KBr is slightly larger for **II**, about the same for **III**, and only one-half of those in KBr for **IV** (Table 2). These ratios suggest ill-defined SAMs with probable multiple orientations. The peak

TABLE 1: Peak Assignments for Furan-containing Oligoaryls in KBr Pellets and in Monolayers Mixed with Dodecanethiol

peak position (cm^{-1})			
in KBr	in mixed monolayers	vibrational mode[b]	transition dipole direction[c]
3052	- - -[a]	ν_{2a}(CH), in-plane stretching	phenyl ring:[d] **a₁**
2965	2963	$\nu_a(CH_3$, ip), asym stretching	
2933	2937	$\nu_s(CH_3$, FR), sym stretching	
- - -[a]	2920	$\nu_a(CH_2)$, asym stretching	
2868	2871	$\nu_s(CH_3)$, sym stretching	
2859	2860	$\nu_s(CH_2)$, sym stretching	
2567	- - -[a]	ν(SH)	
1607	1603	ν_{8a}(C═C), in-plane stretching	phenyl ring:[d] **a₁**
1508	1504−1491	ν_{19a}(C═C), in-plane stretching ν(C═C), in-plane ring stretching	phenyl ring:[d] **a₁** furan:[e] $\mathbf{A}_1$, $\parallel C_{2v}$ axis
1465	1465	$\delta(CH_2)$), deformation	
1250	1265	δ(CH), in-plane bending	furan:[e] $\mathbf{B}_1$, $\perp C_{2v}$ axis
1180	1180	ν_{19a}(C═C), in-plane stretching δ(CH), in-plane bending	phenyl ring:[d] **a₁** furan:[e] $\mathbf{B}_1$, $\perp C_{2v}$ axis
1107	1106	ν_{18b}(CH), in-plane bending	phenyl ring:[d] **b₂**
1060	1041	δ(CH), in-plane bending	furan:[e] $\mathbf{A}_1$, $\parallel C_{2v}$ axis
833	820	ν_{10a}(CH), out-of-plane bending	phenyl ring:[d] **a₂**

[a] The peak intensity is negligible. [b] Subscripts: a, asymmetric; s, symmetric; numbers, modes defined in ref 69. [c] The directions of the transition dipoles with respect to the molecule plane are depicted in Figure 2. [d] Ref 69. [e] Ref 67.

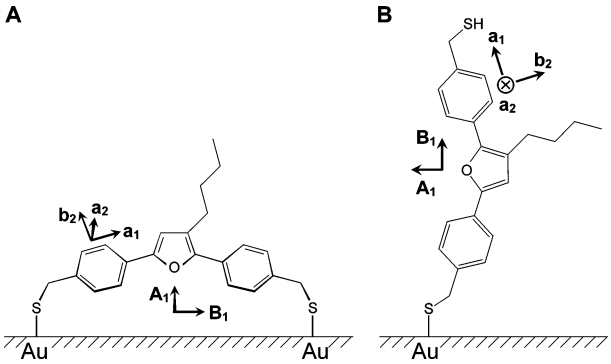

Figure 2. Proposed binding schemes for **III** self-assembly and corresponding vibrational modes for *para*-benzene and furan moieties.

intensity of $\mathbf{a_2}$ mode (out-of-plane) at 820 cm^{-1} is distinct, indicative of a large tilting angle of the phenyl rings away from the surface normal. Most likely, although the furan-containing oligoaryls on gold adopt a preferential orientation resembling Figure 2A, the packing is disordered in nature, consistent with the mobility measurements for **I** (vide supra).[24]

Panels G, H, and I of Figure 1 are typical IRAS spectra of mixed monolayers prepared by immersing substrates of preassembled *n*-dodecanethiol SAMs into the oligoaryl deposition solutions. For mixed monolayers of **II**/dodecanethiol SAMs, the out-of-plane band $\mathbf{a_2}$ becomes indistinct and the intensity ratios of $I_{\mathbf{b2}}/I_{\mathbf{a1}}$ at 1603 cm^{-1} (Table 2) and $I_{\mathbf{A1}}/I_{\mathbf{B1}}$ are smaller than those in KBr, suggesting an orientation similar to that of Figure 2B for **II** (monothiol). However, no lattice structure was found by STM (vide infra). For **III** and **IV**, the ratios of $I_{\mathbf{b2}}/I_{\mathbf{a1}}$, $I_{\mathbf{A1}}/I_{\mathbf{B1}}$, and $I_{\mathbf{b2}}/I_{\mathbf{a1}+\mathbf{B1}}$ at 1180 cm^{-1} for the mixed monolayer are evidently larger than those in KBr pellets and in single-component monolayers. The attenuation in peak ratios supports the formation of the structure shown in Figure 2A and rules out the possibility of Figure 2B, which would require that the ratios of $I_{\mathbf{b2}}/I_{\mathbf{a1}}$ and $I_{\mathbf{b2}}/I_{\mathbf{a2}}$ be smaller than those in KBr pellets. The out-of-plane mode ($\mathbf{a_2}$ at 820 cm^{-1}) becomes very small in Figure 1H and still significant in Figure 1I, suggesting that the molecular tilt angle of the phenyl rings for **III** is smaller that that of **IV**. Taken together, the spectra indicate a better uniformity of the molecular orientation in mixed monolayers than that in single-component films.

STM Measurements. Numerous attempts in adjusting deposition time, concentrations of **II**−**IV**, and solvent selection have been carefully carried out. However, STM provides no indication that the single-component SAMs are well-ordered nor exhibit well-defined stacking of oligoaryls even within small domains, suggesting ill crystallinity for the branched furan oligoaryls on gold substrate. Mixed monolayers of monothiol **II**/dodecanethiol do not show lattice packing of **II** by STM. Surprisingly, images of well-ordered structures for striped **III** and **IV** domains can be found in mixed monolayers (Figure 3). Although missing row and low-density SAMs of *n*-alkanethiol exhibit pinstriped phases, this is unlikely the case on the basis of the assessment stated in the following. First, the unit-cell symmetry for these missing row and low-density *n*-alkanethiol SAMs is close to rectangular,[80−84] different than those of **III** and **IV** whose angles between the unit cell vectors are 60° and 76°, respectively. Literature of low-density *n*-dodecanethiol SAMs is rare. Godin et al. recently reported a stacked lying-down structure for low-density *n*-dodecanethiol SAMs.[85] The length of the observed stripe is 1.5 nm,[85] significantly smaller than our findings for crystalline domains of **III** and **IV** (vide infra). Second, spectra of STS (scanning tunneling spectroscopy) for the striped **III** and **IV** domains are distinct from those for the *n*-dodecanethiol matrix. The STS spectra are provided in the supporting material because the results are not pertinent to this present study and the detailed investigations of STS for the branched furan oligoaryls are still ongoing. Third, we did parallel experiments that, under the same conditions as those for preparing striped **III** and **IV** domains, the preassembled *n*-dodecanethiol SAMs were re-immersed in either monothiol **II** or THF blank solution. Striped features such as those of crystalline **III** and **IV** domains were not found.

Panels A, B, and C of Figure 3 are STM images of **III**/dodecanethiol mixed monolayers; panel D is obtained from SAMs containing **IV**. The upper part of Figure 3A and the lower part of Figure 3B show large domains of c(4 × 2), characteristic of *n*-alkanethiol SAMs on Au(111).[86,87] Around domain boundaries at the lower left corner of panel A and the upper part of panel B, the images reveal packing of **III**. The stacking pattern is different from that of the c(4 × 2) and exhibits a 3-fold symmetry (inset of panel A). The inset of panel B is an enlarged view of the c(4 × 2) structure of dodecanethiol. Because of the

TABLE 2: Relative Intensities of Representative Vibrational Modes of II−IV in KBr Pallets and in Monolayers

	peak intensity ($\times 10^4$ arbitrary unit) and **intensity ratio**								
	compound **II**			compound **III**			compound **IV**		
		monolayers			monolayers			monolayers	
vibrational mode	in KBr	**II** only[a]	mixed[b]	in KBr	**III** only[a]	mixed[b]	in KBr	**IV** only[a]	mixed[b]
$\mathbf{b_2}$ (1106 cm^{-1})	1489.2	3.3	3.1	208.4	6.1	6.8	743.3	6.8	7.9
$\mathbf{a_1}$ (1603 cm^{-1})	1945.1	3.1	6.2	188.0	6.7	2.4	662.5	13.1	1.5
I_{b2}/I_{a1}	0.77	1.1	0.50	1.1	0.91	2.8	1.1	0.52	5.3

[a] Single-component monolayers. [b] Assembled on dodecanethiol-preadsorbed monolayers.

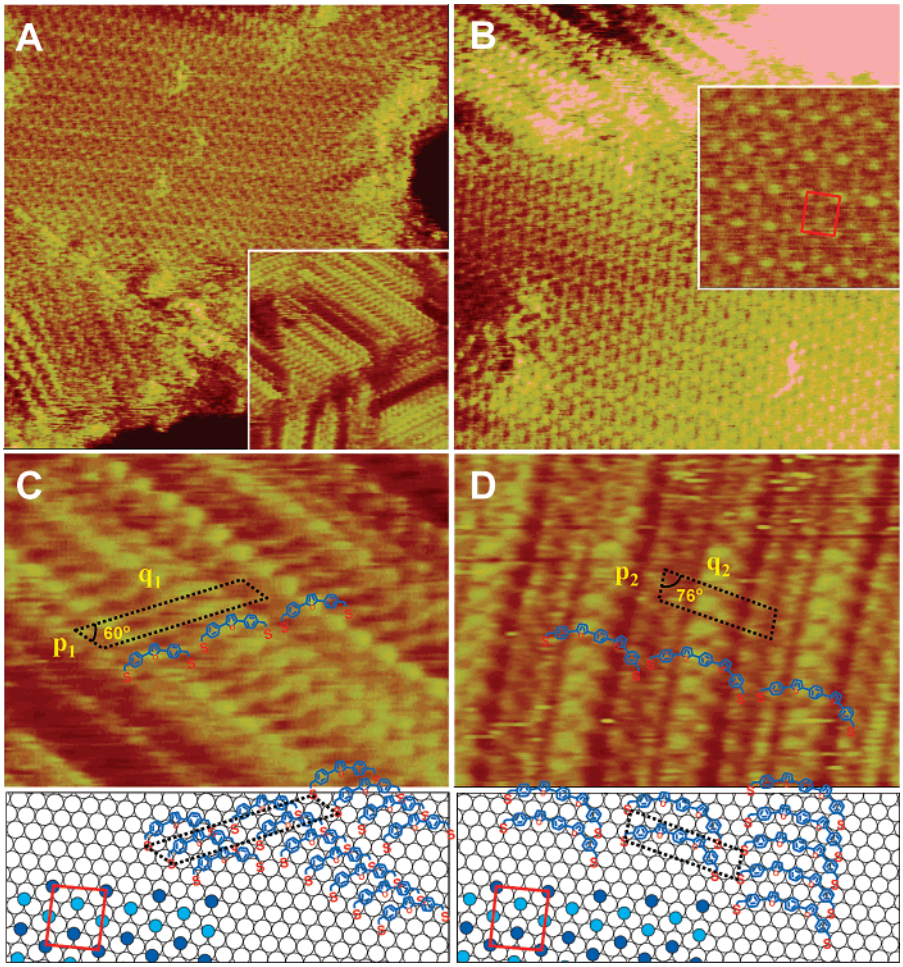

Figure 3. STM images of mixed monolayers of (A−C) **III** and *n*-dodecanethiol, (D) **IV** and *n*-dodecanethiol on Au(111). Imaging size: (A) 30 nm × 30nm, (B) 20 nm × 20nm, (C) 8.5 nm × 6.5 nm, and (D) 8.5 nm × 6.5 nm; typical imaging conditions: V_{bias}, 1.4 V; i_t, 12 pA. The inset in (A) shows the image of three domains of **III**, imaging size: 17 nm × 17 nm. The inset in (B) magnifies the characteristic c(4 × 2) unit cell of *n*-dodecanethiol SAMs. The bottom parts of (C) and (D) illustrate proposed packing structures of dodecanethiol, **III**, and **IV**. The *n*-butyl group is omitted for clarity. Note that, for **III** (C), one thiol is designated to lodge at a 3-fold hollow site while the other at a bridging site. Other arrangements with the sulfur atoms in the 3-fold hollow, bridging, or ontop sites are also possible.

well-established correlation of the c(4 × 2) unit cell with respect to that of the underlayer Au(111), the angles of unit cell vectors of c(4 × 2) relative to those of **III** and **IV** lead us to deduce their lattice structures on Au(111). Higher magnified images for **III** and **IV** stacking are presented in panels C and D of Figure 3. Position of the butyl cannot be identified because of its fluxional nature at room temperature. The nominal width of the stripes in panels C and D (i.e., $|\mathbf{q_1}|$ and $|\mathbf{q_2}|$ in Figure 3) are 2.50 and 2.02 nm, which correlate well with the length of the corresponding molecules and are, respectively, equivalent to $5\sqrt{3}$ and $4\sqrt{3}$ times gold diameter. Along the direction of **p**, the molecules do not exhibit modulation in height, and the respective spacings for **III** and **IV** are 0.51 ± 0.03 nm, consistent with $\sqrt{3}$ times the Au spacing. In consequence, vector **p** is commensurate with the ⟨121⟩ direction of Au(111). The models shown in panels C and D are a $(\sqrt{3} \times 5\sqrt{3})$ structure for **III** and a $(\sqrt{3} \times 4\sqrt{3})$ for **IV** where the angles between the unit cell vectors (**p** and **q**) are ca. 60° and 76°, respectively. At the bottom parts of the images are the proposed models of molecular stacking and unit cells that illustrate the reason the images appear curvy and alternating with bright and dark rolls. This feature is ascribed to the arch-shaped conformation of the furan-containing oligoaryls where the central part is higher than the arms (Chart 2 and Figure 2A).

Discussion

In the study of single-component monolayers of furan-containing oligoaryls, results of FTIR and STM imaging unveil

SCHEME 1

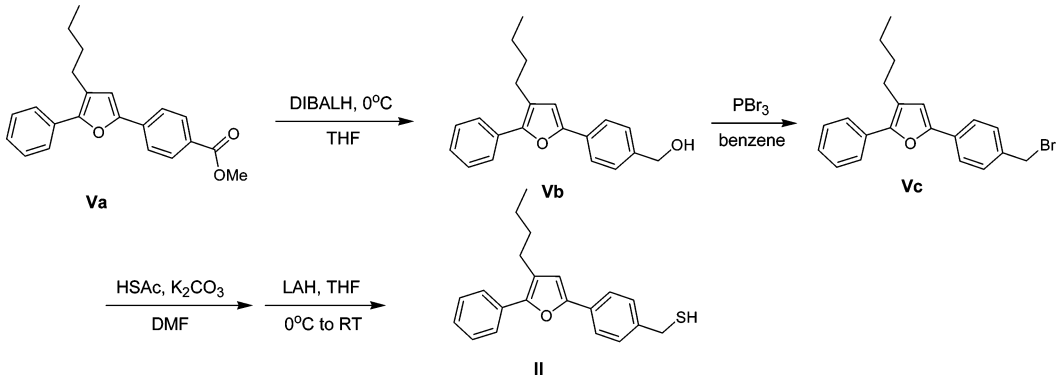

disordered molecular monolayers, demonstrating that the steric effect arising from the butyl group and the arched molecular shape are the dominant factors on monolayer structures even though the intermolecular attractions are contributed from as many as 5 aromatic rings. The finding reconfirms our previous analysis that the thin films of these oligoaryls are not crystalline and are suitable for OLED devices.[23,24]

We manage to obtain crystalline domains of **III** and **IV** by exposing preassembled *n*-dodecanethiol SAMs in the corresponding deposition solutions. Several novel and intriguing findings are discovered: (1) the stacking features of **II**−**IV** cannot be found without the presence of dodecanethiol SAMs, (2) the long axes of the molecules and their aryl planes are, respectively, perpendicular to and slightly tilted away from the surface normal, an unprecedented packing structure in exclusively upright ω-dithiol aromatic SAMs,[31,32,55] and (3) the domains are small and appeared to reside against the well-defined c(4×2) of *n*-dodecanethiol SAMs.

The assembly of the stacking features should take place during the exchange of dodecanethiol by **III** and **IV** because of the absence of in-film crystallinity for single-component SAMs. This assembling process is in essence the same as mixed-monolayer preparation, where surface-bound thiols are displaced by excess free thiols in solution. In literature reports, such exchange reactions are generally associated with a fast and a slow step although the experimental conditions are very different in molar ratios of free to surface-bound molecules and in properties of solvents and molecules.[88−90] The fast step takes place at defects, such as domain boundaries of the alkanethiol SAMs, where free thiols can reach the gold surface relatively easily. At terraces or domains where the molecules are tightly packed, the kinetics is so slow that the exchange remains incomplete for reactions taking longer than 10 days.[88−90] Accordingly, the packing stripes of **III** and **IV** are situated against the c(4×2) domain of dodecanethiol SAMs.

Why and how do the preassembled dodecanethiol SAMs assist the stacking of **III** and **IV**? The arched shape of **III** and **IV** allows them to bind on gold substrate with two thiol legs. In the case of single-component SAMs, the oligoaryls chemisorb readily on bare gold because of the ease in developing the S−Au bond. The promptness of chemisorption generates chaotically distributed monolayers in which the arched molecules hinge each other and block the desorptive pathways. It is difficult for the dithiols to simultaneously break two S−Au bonds, to desorb, and then to readsorb, the key step of refining the intermolecular attractions for crystalline monolayers.[36,41] Consequently, the steric effect of the branched furan oligoaryls governs the developed structures. In the case of mixed monolayers, the adsorption rate of **III** and **IV** is regulated by the slow desorption of dodecanethiols at domain boundaries. The adsorption sites are confined in a limited area where the furan-containing oligoaryls are unlikely to be jam-packed and, nonetheless, provides a sufficient space to maneuver the thiol legs to a thermodynamically favorable location. In the process of repetitively exchanging dodecanethiol and the dithiols (**III** and **IV**) within a confined space, the $\pi-\pi$ attractions of the aromatics become dominant and generate the stripe stacking whose butyl groups no longer impose steric hindrance.

In summary, we have shown that the one-pot strategy starting from propargylic dithioacetals can successfully synthesize thiolated furan-containing oligoaryls (**II**−**IV**). General procedures of preparing SAMs by soaking substrates in the deposition solutions result in ill-defined SAMs. The lack of lattice structure is attributed to the steric side chain, the rigid and arched molecular geometry, and the dithiol legs, which require simultaneous desorption of the thiolates and make it difficult to improve the intermolecular attractions. By preassembling *n*-dodecanethiol SAMs, the space for the furan-containing oligoaryls to reside is limited to domain boundaries where crystalline packing of **III** and **IV** can grow.

Experimental Section

Chemical Materials. All chemicals were used as received unless otherwise noted. The synthetic procedures for compounds **II**−**IV** are described in the following where the starting materials were prepared on the basis of those reported previously.[19−24]

Synthesis of Teraryl-mono-thiol (II). *Teraryl-mono-ol (Vb).* Under argon atmosphere, a THF solution (60 mL) of **Va** (1.25 g, 3.7 mmol) was treated with DIBALH (16.0 mL of 1.0 M solution, 16.0 mmol) at 0 °C. The mixture was stirred for 30 min at 0 °C and was gradually warmed to room temperature and stirred for 5 h. After quenching with 10% NH_4Cl (10 mL) and extracted with ether, the organic layer was dried with $MgSO_4$, and then the solvent was removed in vacuo. The residue material was recrystallized from CH_2Cl_2-hexane to give the **Vb** (903 mg, 79%) mp 65−66 °C: ^{1}H NMR (300 MHz, $CDCl_3$) δ 0.95 (t, $J = 7.4$ Hz, 3 H), 1.43 (sextet, $J = 7.4$ Hz, 2 H), 1.66 (tt, $J = 7.7$, 7.4 Hz, 2 H), 2.69 (t, $J = 7.7$ Hz, 2 H), 4.70 (d, $J = 5.7$ Hz, 2 H), 6.65 (s, 1 H), 7.29 (t, $J = 7.7$ Hz, 1 H), 7.38 (t, $J = 7.7$ Hz, 2 H), 7.44 (d, $J = 7.7$ Hz, 2 H), 7.67 (d, $J = 7.5$ Hz, 2 H), 7.70 (d, $J = 7.5$ Hz, 2 H). ^{13}C NMR (125 MHz, $CDCl_3$) δ 14.0, 22.6, 25.7, 32.1, 65.2, 109.3, 123.8, 124.1, 125.5, 126.8, 127.4, 128.6, 130.3, 131.7, 139.7, 148.0, 151.6. IR (KBr) ν 3327, 3079, 2949, 2928, 2849, 1594, 1500, 1484, 1464, 1421, 1282, 1186, 1044, 934, 809, 763, 694, 667, 508, 483 cm^{-1}. HRFAB calcd for $C_{21}H_{22}O_2$ 306.1620, found 306.1615. Anal. Calcd for $C_{21}H_{22}O_2$ C, 82.32; H, 7.24. Found C, 81.79; H, 7.15.*Teraryl-mono-bromide (Vc).* Under argon atmosphere, a

benzene solution (10 mL) of **Vb** (0.61 g, 2.0 mmol) and PBr_3 (d = 2.88, 0.2 mL, 2.1 mmol) was stirred for 12 h at room temperature. The mixture was treated with 10% $NaHCO_3$ (5 mL) and extracted with CH_2Cl_2. The organic layer was dried ($MgSO_4$), and then the solvent was removed in vacuo. The residue was recrystallized from hexane-CH_2Cl_2 to give the **Vc** (570 mg, 79%) mp 79−80 °C: ^{1}H NMR (400 MHz, $CDCl_3$) δ 0.94 (t, J = 7.4 Hz, 3 H), 1.49 (sextet, J = 7.4 Hz, 2 H), 1.72 (tt, J = 7.8, 7.4 Hz, 2 H), 2.75 (t, J = 7.8 Hz, 2 H), 4.59 (s, 2 H), 6.78 (s, 1 H), 7.34 (tt, J = 7.4, 1.4 Hz, 1 H), 7.42−7.55 (m, 4 H), 7.70−7.80 (m, 4 H). ^{13}C NMR (125 MHz, $CDCl_3$) δ 14.0, 22.6, 25.7, 32.1, 33.6, 109.9, 123.9, 124.2, 125.6, 126.9, 128.6, 129.5, 130.9, 131.6, 136.4, 148.3, 151.3. IR (KBr) ν 3055, 2951, 2927, 2858, 1611, 1499, 1484, 1464, 1443, 1420, 1224, 1197, 1091, 1057, 934, 838, 813, 761, 688, 667, 596 cm^{-1}. HRFAB calcd for $C_{21}H_{21}{}^{79}BrO$ 368.0776, found 368.0772. Anal. Calcd for $C_{21}H_{21}BrO$ C, 68.30; H, 5.73. Found C, 67.86; H, 6.01.

Teraryl-mono-thiol (II). To a solution of K_2CO_3 (207 mg, 1.5 mmol) in DMF (4 mL) was slowly added a solution of freshly distilled thioacetic acid (0.1 mL, 1.5 mmol) in DMF (2 mL). After 10 min, this solution was added to a solution of **Vc** (360 mg, 1.0 mmol) in DMF (4 mL), and then the mixture was stirred overnight under the exclusion of light. After removal of solvent, the residue was dissolved in CH_2Cl_2 (20 mL) and washed with water and brine. The organic layer was dried ($MgSO_4$), and then the solvent was removed in vacuo. The residue (232 mg, 0.64 mmol) in THF (6 mL) was allowed to react with LAH (38 mg, 1.0 mmol) in THF (6 mL) solution at 0 °C for 10 min, then warmed to room temperature and stirred for an additional 30 min. The mixture was cooled to 0 °C and then treated with 3 N aqueous HCl under an argon atmosphere until all the solid had dissolved. The biphasic mixture was diluted with ether (20 mL) and water (20 mL). The organic layer was dried ($MgSO_4$), removed in vacuo, and the residue was chromatographed (silica gel, CH_2Cl_2/hexane) to give **II** (267 mg, 83% for two steps): ^{1}H NMR (300 MHz, $CDCl_3$) δ 0.94 (t, J = 7.4 Hz, 3 H), 1.43 (sextet, J = 7.4 Hz, 2 H), 1.66 (tt, J = 7.7 Hz, 7.4 Hz, 2 H), 1.76 (t, J = 7.4 Hz, 1 H), 2.68 (t, J = 7.7 Hz, 2 H), 7.74 (d, J = 7.4 Hz, 2 H), 6.63 (s, 1 H), 7.26 (t, J = 7.8 Hz, 1 H), 7.32 (d, J = 7.8 Hz, 2 H), 7.42 (t, J = 7.8 Hz, 2 H), 7.65 (d, J = 7.7 Hz, 2 H), 7.67 (d, J = 7.7 Hz, 2 H). ^{13}C NMR (75 MHz, $CDCl_3$) δ 13.9, 22.6, 25.7, 28.8, 32.1, 109.2, 124.0, 124.1, 125.5, 126.8, 128.4, 128.5, 129.7, 131.8, 140.0, 148.0, 151.6. IR (KBr) ν 3026, 2955, 2928, 2869, 2859, 2567, 1605, 1597, 1500, 1486, 1465, 1251, 1182, 1109, 1073, 1051, 933, 839, 811, 692 cm^{-1}. HRFAB calcd for $C_{21}H_{22}OS$ 322.1391, found 322.1388. Anal. Calcd for $C_{21}H_{22}OS$ C, 78.22; H, 6.88. Found C, 77.99; H, 7.10.

Synthesis of Ter- or Penta-aryl-bis-dithiol (III or IV). *Ter- or Penta-aryl-bis-diol (VIb or VIIb).* Under argon atmosphere, a THF solution (60 mL) of **VIa** or **VIIa** (1.0 mmol) was treated with DIBALH (8.0 mL of 1.0 M solution, 8.0 mmol) at 0 °C and stirred for 30 min. The mixture was stirred for 30 min at 0 °C and was gradually warmed to room temperature and then stirred for 5 h. After quenching with 10% NH_4Cl (10 mL) and extracted with ether, the organic layer was dried ($MgSO_4$), and the solvent was removed in vacuo. The residue material was recrystallized from CH_2Cl_2-hexane to give the alcohol **VIb** (312 mg, 93%) or **VIIb** (486 mg, 91%).**VIb** mp 113−114 °C: ^{1}H NMR (400 MHz, $CDCl_3$) δ 0.94 (t, J = 7.4 Hz, 3 H), 1.42 (sextet, J = 7.4 Hz, 2 H), 1.65 (tt, J = 7.4, 7.8 Hz, 2 H), 2.04 (br, 2 H), 2.66 (t, J = 7.8 Hz, 2 H), 4.65 (s, 2 H), 4.68 (s, 2 H), 6.63 (s, 1 H), 7.34 (d, J = 8.2 Hz, 2 H), 7.39 (d, J = 8.2 Hz, 2 H), 7.65 (d, J = 8.2 Hz, 2 H), 7.67 (d, J = 8.2 Hz, 2 H). ^{13}C NMR (100 MHz, $CDCl_3$) δ 13.9, 22.6, 25.7, 32.0, 65.0, 109.2, 123.8, 124.2, 125.6, 127.2, 127.3, 130.1, 131.1, 139.3, 139.7, 147.7, 151.6.

CHART 3

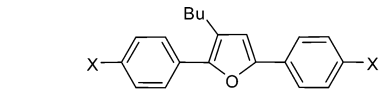

VI

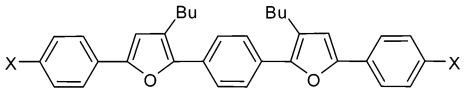

VII

VIa, VIIa, X = CO_2Me
VIb, VIIb, X = CH_2OH
VIc, VIIc, X = CH_2Br
VId, VIId, X = CH_2SAc
III, IV, X = CH_2SH

VIIb mp 170−171 °C: ^{1}H NMR (300 MHz, $CDCl_3$) δ 0.97 (t, J = 7.3 Hz, 6 H), 1.46 (sextet, J = 7.3 Hz, 4 H), 1.68 (s, 2 H), 1.69 (quint, J = 7.6 Hz, 4 H), 2.73 (t, J = 7.6 Hz, 4 H), 4.70 (s, 4 H), 6.67 (s, 2 H), 7.38 (d, J = 8.2 Hz, 4 H), 7.71 (d, J = 8.2 Hz, 4 H), 7.75 (s, 4 H). ^{13}C NMR (100 MHz, $CDCl_3$) δ 14.0, 22.7, 25.9, 32.1, 65.2, 109.5, 123.9, 124.5, 125.5, 127.4, 130.0, 130.2, 139.8, 147.8, 151.7.

Ter- or Penta-aryl-bis-dibromide (VIc or VIIc). Under argon atmosphere, a benzene solution (10 mL) of **VIb** or **VIIb** (1.0 mmol) and PBr_3 (d = 2.88, 0.2 mL, 2.1 mmol) was stirred for 12 h. The mixture was treated with 10% $NaHCO_3$ (5 mL) and extracted with CH_2Cl_2. The organic layer was dried ($MgSO_4$), and the solvent was removed in vacuo. The residue was recrystallized from hexane-CH_2Cl_2 to give **VIc** (432 mg, 94%) or **VIIc** (612 mg, 93%).

VIc mp 116−117 °C: ^{1}H NMR (300 MHz, $CDCl_3$) δ 0.97 (t, J = 7.3 Hz, 3 H), 1.23 (sextet, J = 7.3 Hz, 2 H), 1.64 (tt, J = 7.7, 7.3 Hz, 2 H), 2.70 (t, J = 7.7 Hz, 2 H), 4.52 (s, 2 H), 4.54 (s, 2 H), 6.68 (s, 1H), 7.42 (d, J = 8.3 Hz, 2 H), 7.45 (d, J = 8.3 Hz, 2 H), 7.66 (d, J = 8.2 Hz, 2 H), 7.68 (d, J = 8.2 Hz, 2 H). ^{13}C NMR (75 MHz, $CDCl_3$) δ 14.0, 22.6, 25.8, 32.0, 33.5, 70.8, 110.0, 124.0, 125.0, 125.7, 129.4, 129.5, 130.7, 131.7, 136.1, 136.6, 147.7, 151.6. IR (KBr) ν 2959, 2932, 2862, 1614, 1511, 1228, 1203, 1096, 935, 841, 817, 601 cm^{-1}. HRFAB calcd for $C_{22}H_{22}Br_2O$ 460.0037, found 460.0044.

VIIc mp 185−187 °C: ^{1}H NMR (300 MHz, $CDCl_3$) δ 0.99 (t, J = 7.2 Hz, 6 H), 1.47 (sextet, J = 7.2 Hz, 4 H), 1.70 (tt, J = 7.6, 7.2 Hz, 4 H), 2.75 (t, J = 7.6 Hz, 4 H), 4.54 (s, 4 H), 6.71 (s, 2H), 7.42 (d, J = 8.1 Hz, 4 H), 7.70 (d, J = 8.1 Hz, 4 H), 7.77 (s, 4 H). ^{13}C NMR (75 MHz, $CDCl_3$) δ 14.0, 22.6, 25.9, 32.0, 33.6, 110.1, 123.9, 124.6, 125.5, 129.5, 129.9, 130.8, 136.5, 148.0, 151.3. IR (KBr) ν 2960, 2932, 2873, 1611, 1510, 1460, 1226, 1200, 1090, 934, 840, 814, 672, 596 cm^{-1}. HRFAB calcd for $C_{36}H_{36}Br_2O_2$ 658.1082, found 658.1072.

Ter- or Penta-aryl-bis-dithioacetate (VId or VIId). To a solution of K_2CO_3 (3.0 mmol) in DMF (10 mL) was slowly added a solution of freshly distilled thioacetic acid (0.2 mL, 3.0 mmol) in DMF (5 mL). After 10 min, this solution was added to a solution of **VIc** or **VIIc** (1.0 mmol) in DMF (10 mL), and the mixture was stirred overnight under the exclusion of light. After removal of solvent, the residue was dissolved in CH_2Cl_2 (40 mL) and washed with water and brine. The organic layer was dried ($MgSO_4$), the solvent was removed in vacuo, and the residue was chromatographed (silica gel, EtOAc/hexane) to give **VId** (407 mg, 90%) or **VIId** (598 mg, 92%).

VId: ^{1}H NMR (300 MHz, $CDCl_3$) δ 0.93 (t, J = 7.2 Hz, 3 H), 1.40 (sextet, J = 7.2 Hz, 2 H), 1.63 (tt, J = 7.7, 7.2 Hz, 2 H), 2.34 (s, 3 H), 2.35 (s, 3 H), 2.64 (t, J = 7.7 Hz, 2 H), 4.11 (s, 2 H), 4.13 (s, 2 H), 6.60 (s, 1 H), 7.25 (d, J = 8.2 Hz, 2 H), 7.30 (d, J = 8.2 Hz, 2 H), 7.58 (d, J = 8.0 Hz, 2 H), 7.60 (d, J = 8.0 Hz, 2 H). ^{13}C NMR (75 MHz, $CDCl_3$) δ 13.9, 22.6, 22.7, 25.7, 30.2, 30.3, 32.0, 33.2, 33.3, 41.2, 109.3, 123.8, 124.2, 125.6, 129.0, 129.8, 130.7, 136.0, 136.4, 147.6, 151.5, 195.0. IR (KBr) ν 2959, 2931, 2866, 1692, 1655, 1509, 1134, 1104, 958, 626 cm^{-1}; HRFAB calcd for $C_{26}H_{18}O_3S_2$ 452.1480, found 452.1483.

VIId mp 142−143 °C: ^{1}H NMR (300 MHz, $CDCl_3$) δ 0.98 (t, J = 7.3 Hz, 6 H), 1.48 (sextet, J = 7.3 Hz, 4 H), 1.68 (tt, J = 7.7, 7.3 Hz, 4 H), 2.37 (s, 6 H), 2.74 (t, J = 7.7 Hz, 4 H), 4.14 (s, 4 H), 6.66 (s, 2 H), 7.31 (d, J = 8.2 Hz, 4 H), 7.66 (d, J = 8.2 Hz, 4 H), 7.75 (s, 4 H). ^{13}C NMR (75 MHz, $CDCl_3$) δ 14.0, 22.6, 25.9, 30.4, 32.1, 33.3, 109.5, 123.9, 124.5, 125.4, 129.2, 129.8, 129.9, 136.5, 147.7, 151.6, 195.1. IR (KBr) ν 2952, 2924, 2860, 2568, 1685, 1510, 1488, 1137, 936, 834, 755, 670, 635 cm^{-1}. HRFAB calcd for $C_{40}H_{42}O_4S_2$ 650.2525, found 650.2520.

Ter- or Penta-aryl-bis-dithiol (III or IV). Under argon atmosphere, a THF solution (10 mL) of LAH (3 equiv) was treated with THF solution (10 mL) of **VId** or **VIId** (1.0 mmol) at 0 °C, and stirred for 10 min, then warmed to room temperature and stirred an additional 30 min. The mixture was cooled to 0 °C and treated with 3 N aqueous HCl under an argon atmosphere until all the solid had dissolved. The biphasic mixture was diluted with ether (20 mL) and water (20 mL). The organic layer was dried ($MgSO_4$), removed in vacuo, and the residue was chromatographed (silica gel, CH_2Cl_2/hexane) to give **III** (305 mg, 83%) or **IV** (453 mg, 80%).

III: ^{1}H NMR (200 MHz, $CDCl_3$) δ 0.96 (t, J = 7.2 Hz, 3 H), 1.45 (sextet, J = 7.2 Hz, 2 H), 1.65 (tt, J = 7.6, 7.2 Hz, 2 H), 1.78 (t, J = 7.5 Hz, 1 H), 1.80 (t, J = 7.5 Hz, 1 H), 2.69 (t, J = 7.6 Hz, 2 H), 3.76 (d, J = 7.5 Hz, 2 H), 3.78 (d, J = 7.5 Hz, 2 H), 6.65 (s, 1 H), 7.34 (d, J = 8.2 Hz, 2 H), 7.38 (d, J = 8.2 Hz, 2 H), 7.65 (d, J = 8.1 Hz, 2 H), 7.67 (d, J = 8.1 Hz, 2 H). ^{13}C NMR (100 MHz, $CDCl_3$) δ 14.0, 22.6, 25.8, 28.80, 28.82, 32.1, 109.2, 123.9, 124.2, 125.7, 128.3, 129.6, 130.6, 139.6, 140.0, 147.7, 151.6. IR (KBr) ν 3030, 2959, 2931, 2872, 2862, 2568, 1607, 1510, 1494, 1252, 1104, 1052, 935, 841, 813 cm^{-1}. HRFAB calcd for $C_{22}H_{24}OS_2$ 368.1269, found 368.1277. Anal. Calcd for $C_{22}H_{24}OS_2$ C, 71.69; H, 6.56. Found C, 71.47; H, 6.22.

IV mp 125−129 °C: ^{1}H NMR (400 MHz, $CDCl_3$) δ 0.96 (t, J = 7.3 Hz, 6 H), 1.45 (sextet, J = 7.3 Hz, 4 H), 1.68 (tt, J = 7.7, 7.3 Hz, 4 H), 1.76 (t, J = 7.5 Hz, 2 H), 2.72 (t, J = 7.7 Hz, 4 H), 3.75 (d, J = 7.5 Hz, 4 H), 6.65 (s, 2 H), 7.33 (d, J = 8.3 Hz, 4 H), 7.66 (d, J = 8.3 Hz, 4 H), 7.74 (s, 4 H). ^{13}C NMR (75 MHz, $CDCl_3$) δ 14.0, 22.6, 25.9, 28.8, 32.1, 109.4, 123.9, 124.5, 125.4, 128.4, 129.6, 129.9, 140.0, 147.7, 151.6. IR (KBr) ν 3023, 2956, 2927, 2868, 2857, 2562, 1607, 1598, 1509, 1486, 1250, 1190, 1104, 1060, 1019, 933, 833, 814, 794, 669 cm^{-1}. HRFAB calcd for $C_{40}H_{42}O_4S_2$ 566.2313, found 566.2311.

Preparation of Monolayers. The deposition solutions contained 0.24 mM thiolated furan oligoaryls (**II**−**IV**) in THF. To prepare monolayers containing a single component, the soaking time of the gold substrate was ranging from 3 h to days. The sample was rinsed thoroughly in sequence with THF and ethanol. To remove trace amount of solvent, the sample was subjected to vacuum drying (~30 min, 120 mTorr) prior to STM or IR measurements. To prepare mixed monolayers, the substrates were preassembled with *n*-dodecanethiol (1 mM in EtOH, 80 min ~12 h). After rinsed thoroughly with ethanol, the substrates were treated with the same way as those for single-component SAMs.

STM Measurements. The Au(111) substrates (Gold Arrandee, purchased from Metallhandel Schroer GmbH, Germany) were ~200−300 nm thick gold films with a ~1−4 nm thick Cr adhesive layer and were flame annealed a few times before each experiment. STM measurements were carried out with a NanoScope IIIa (Veeco Metrology Group, Santa Barbara, CA) using a low-current modulus. Commercial Pt/Ir tips (Nanotips, Digital Instruments, Santa Barbara, CA) were employed. Typical imaging conditions of tunneling current and bias voltage were ranging from 10 to 15 pA and from 1.2 to 2 V, respectively. The microscope was housed in a chamber where dry N_2 was purging throughout the experiments and the humidity was lower than 2%.

IR Characterization. Transmission IR spectra of Compounds **II**−**IV** were obtained by KBr-pelleted samples. For IRAS (infrared reflection−absorption spectroscopy) spectra of monolayer films, the substrates were 200-nm-thick gold films thermally evaporated onto glass slides precleaned with piranha solution, a 1:3 (v/v) mixture of 30% H_2O_2 and concentrated H_2SO_4. *This solution reacts violently with organic materials and should be handled with great care*. The pressure in the bell-jar evaporator (Auto 306, Edwards High Vacuum International, West Sussex, UK) was nominally 2×10^{-6} Torr. A 5-nm Cr underlayer was used to enhance the adhesion of the gold film. IRAS spectroscopy was carried out with a Perkin-Elmer System 2000 infrared spectrometer equipped with an MCT detector cooled with liquid nitrogen. The measurement scheme[78] was a single reflection mode and the *p*-polarized light was incident at 85° from the surface normal with a grazing angle accessory (FT-85, Spectra-Tech, Shelton, CT). The light path, detector, and sample chambers were purged with dry nitrogen. Both the sample and the reference (bare Au) 1024 scans were collected at 4 cm^{-1} resolution for signal averaging.

Acknowledgment. We thank the National Science Council and the Ministry of Education (Taiwan, R.O.C.) for financial support. We also thank Professor M.-K. Leung for the fruitful discussion of the assembly mechanism of the mixed monolayers.

Supporting Information Available: Preliminary spectra of scanning tunneling spectroscopy for *n*-dodecanethiol SAMs and crystalline domains of **III** and **IV** (Figure S1). This material is available free of charge via the Internet at http://pubs.acs.org.

References and Notes

(1) Mullen, K., Wegner, G., Eds. *Electronic Materials: The Oligomer Approach*; Wiley-VCH: Weinheim, 1998.
(2) Tour, J. M. *Acc. Chem. Res.* **2000**, *33*, 791−804.
(3) Roncali, J. *Chem. Rev.* **1992**, *92*, 711−738.
(4) Martin, R. E.; Diederich, F. *Angew. Chem., Int. Ed.* **1999**, *38*, 1350−1377.
(5) Tour, J. M. *Chem. Rev.* **1996**, *96*, 537−554.
(6) Roncali, J. *Chem. Rev.* **1997**, *97*, 173−206.
(7) Hucke, A.; Cava, M. P. *J. Org. Chem.* **1998**, *63*, 7413−7417.
(8) Dufresne, G.; Bouchard, J.; Belletete, M.; Durocher, G.; Leclerc, M. *Macromolecules* **2000**, *33*, 8252−8257.
(9) Roncali, J. *J. Mater. Chem.* **1997**, *7*, 2307−2321.
(10) Segura, J. L.; Martin, N. *Angew. Chem., Int. Ed.* **2001**, *40*, 1372−1409.
(11) Nielsen, M. B.; Utesch, N. F.; Moonen, N. N. P.; Boudon, C.; Gisselbrecht, J.-P.; Concilio, S.; Piotto, S. P.; Seiler, P.; Gunter, P.; Gross, M.; Diederich, F. *Chem.—Eur. J.* **2002**, *8*, 3601−3613.
(12) Otsubo, T.; Takimiya, K. *Bull. Chem. Soc. Jpn.* **2004**, *77*, 43−58.
(13) Niziurski-Mann, R. E.; Cava, M. P. *Adv. Mater.* **1993**, *5*, 547−551.

(14) Niziurski-Mann, R. E.; Scordilis-Kelley, C.; Liu, T.-L.; Cava, M. P.; Carlin, R. T. *J. Am. Chem. Soc.* **1993**, *115*, 887−891.
(15) Gandini, A.; Belgacem, M. N. *Prog. Polym. Sci.* **1997**, *22*, 1203−1379.
(16) Saadeh, H.; Goodson, T., III.; Yu, L. *Macromolecules* **1997**, *30*, 4608−4612.
(17) Politis, J. K.; Nemes, J. C.; Curtis, M. D. *J. Am. Chem. Soc.* **2001**, *123*, 2537−2547.
(18) Pyo, S. M.; Kim, S. I.; Shim, T. J.; Park, H. K.; Ree, M.; Park, K. H.; Kang, J. S. *Macromolecules* **1998**, *31*, 4777−4781.
(19) Lee, C.-F.; Yang, L.-M.; Hwu, T.-Y.; Feng, A.-S.; Tseng, J.-C.; Luh, T.-Y. *J. Am. Chem. Soc.* **2000**, *122*, 4992−4993.
(20) Liu, C.-Y.; Luh, T.-Y. *Org. Lett.* **2002**, *4*, 4305−4307.
(21) Lee, C.-F.; Liu, C.-Y.; Song, H.-C.; Luo, S.-J.; Tseng, J.-C.; Tso, H.-H.; Luh, T.-Y. *Chem. Commun.* **2002**, 2824−2825.
(22) Tseng, J.-C.; Huang, S.-L.; Tin, C.-L.; Lin, H.-C.; Jin, B.-Y.; Chen, C.-Y.; Yu, J.-K.; Chou, P.-T.; Luh, T.-Y. *Org. Lett.* **2003**, *5*, 4381−4384.
(23) Zhang, L.-Z.; Chen, C.-W.; Lee, C.-F.; Wu, C.-C.; Luh, T.-Y. *Chem. Commun.* **2002**, 2336−2337.
(24) Wu, C.-C.; Hung, W.-Y.; Liu, T.-L.; Zhang, L.-Z.; Luh, T.-Y. *J. Appl. Phys.* **2003**, *93*, 5465−5471.
(25) Schonherr, G.; Bassler, H.; Silver, M. *Philos. Mag. B* **1981**, *44*, 47−61.
(26) Borsenberger, P. M.; Pautmeier, L.; Bassler, H. *J. Chem. Phys.* **1991**, *94*, 5447−5454.
(27) Arkhipov, V. I.; Bassler, H.; Rudenko, A. I. *Philos. Mag. B* **1992**, *65*, 615−619.
(28) Bassler, H. *Phys. Status Solidi B* **1993**, *175*, 15−56.
(29) Borsenberger, P. M.; Weiss, D. S. *Organic Photoreceptors for Imaging Systems*; Marcel Dekker: New York, 1993.
(30) Bassler, H. *Int. J. Mod. Phys. B* **1994**, *8*, 847−854.
(31) de Boer, B.; Meng, H.; Perepichka, D. F.; Zheng, J.; Frank, M. M.; Chabal, Y. J.; Bao, Z. *Langmuir* **2003**, *19*, 4272−4284.
(32) de Boer, B.; Frank, M. M.; Chabal, Y. J.; Jiang, W.; Garfunkel, E.; Bao, Z. *Langmuir* **2004**, *20*, 1539−1542.
(33) Ulman, A. *Chem. Rev.* **1996**, *96*, 1533−1554.
(34) Sabatani, E.; Cohen-Boulakia, J.; Bruening, M.; Rubinstein, I. *Langmuir* **1993**, *9*, 2974−2981.
(35) Tao, Y.-T.; Wu, C.-C.; Eu, J.-Y.; Lin, W.-L.; Wu, K.-C.; Chen, C.-h. *Langmuir* **1997**, *13*, 4018−4023.
(36) Zharnikov, M.; Grunze, M. *J. Phy.: Condens. Matter* **2001**, *13*, 11333−11365.
(37) Yang, G.; Liu, G.-Y. *J. Phys. Chem. B* **2003**, *107*, 8746−8759.
(38) Kang, J. F.; Ulman, A.; Liao, S.; Jordan, R.; Yang, G.; Liu, G.-Y. *Langmuir* **2001**, *17*, 95−106.
(39) Yang, G.; Qian, Y.; Engtrakul, C.; Sita, L. R.; Liu, G.-Y. *J. Phys. Chem. B* **2000**, *104*, 9059−9062.
(40) Xia, Y.; Rogers, J. A.; Paul, K. E.; Whitesides, G. M. *Chem. Rev.* **1999**, *99*, 1823−1848.
(41) Schreiber, F. *Prog. Surf. Sci.* **2000**, *65*, 151−256.
(42) Azzam, W.; Cyganik, P.; Witte, G.; Buck, M.; Woll, Ch. *Langmuir* **2003**, *19*, 8262−8270.
(43) Lin, S.-Y.; Chen, I-W. P.; Chen, C.-h.; Hsieh, M.-H.; Yeh, C.-Y.; Lin, T.-W.; Chen, Y.-H.; Peng, S.-M. *J. Phys. Chem. B* **2004**, *108*, 959−964.
(44) Cyganik, P.; Buck, M.; Azzam, W.; Woll, Ch. *J. Phys. Chem. B* **2004**, *108*, 4989−4996.
(45) Ishida, T.; Mizutani, W.; Aya, Y.; Ogiso, H.; Sasaki, S.; Tokumoto, H. *J. Phys. Chem. B* **2002**, *106*, 5886−5892.
(46) Yang, Y.-C.; Yen, Y.-P.; Ou Yang, L.-Y.; Yau, S.-L.; Itaya, K. *Langmuir* **2004**, *20*, 10030−10037.
(47) Reed, M. A.; Zhou, C.; Muller, C. J.; Burgin, T. P.; Tour, J. M. *Science* **1997**, *278*, 252−254.
(48) Cygan, M. T.; Dunbar, T. D.; Arnold, J. J.; Bumm, L. A.; Shedlock, N. F.; Burgin, T. P.; Jones, L., II; Allara, D. L.; Tour, J. M.; Weiss, P. S. *J. Am. Chem. Soc.* **1998**, *120*, 2721−2732.
(49) Chen, J.; Reed, M. A.; Rawlett, A. M.; Tour, J. M. *Science* **1999**, *286*, 1550−1552.
(50) Chen, J.; Wang, W.; Reed, M. A.; Rawlett, A. M.; Price, D. W., Jr.; Tour, J. M. *Appl. Phys. Lett.* **2000**, *77*, 1224−1226.
(51) Donhauser, Z. J.; Mantooth, B. A.; Kelly, K. F.; Bumm, L. A.; Monnell, J. D.; Stapleton, J. J.; Price, D. W., Jr.; Rawlett, A. M.; Allara, D. L.; Tour, J. M.; Weiss, P. S. *Science* **2001**, *292*, 2303−2307.
(52) Fan, F.-R. F.; Yang, J.; Dirk, S. M.; Price, D. W.; Kosynkin, D.; Tour, J. M.; Bard, A. J. *J. Am. Chem. Soc.* **2001**, *123*, 2454−2455.
(53) Rawlett, A. M.; Hopson, T. J.; Nagahara, L. A.; Tsui, R. K.; Ramachandran, G. K.; Lindsay, S. M. *Appl. Phys. Lett.* **2002**, *81*, 3043−3045.
(54) Fan, F.-R. F.; Yang, J.; Cai, L.; Price, D. W., Jr.; Dirk, S. M.; Kosynkin, D. V.; Yao, Y.; Rawlett, A. M.; Tour, J. M.; Bard, A. J. *J. Am. Chem. Soc.* **2002**, *124*, 5550−5560.
(55) Zhitenev, N. B.; Erbe, A.; Bao, Z. *Phys. Rev. Lett.* **2004**, *92*, 186805/1−186805/4.
(56) Sellers, H.; Ulman, A.; Shnidman, Y.; Eilers, J. E. *J. Am. Chem. Soc.* **1993**, *115*, 9389−9401.
(57) Jung, H. H.; Won, Y. D.; Shin, S.; Kim, K. *Langmuir* **1999**, *15*, 1147−1154.
(58) Szafranski, C. A.; Tanner, W.; Laibinis, P. E.; Garrell, R. L. *Langmuir* **1998**, *14*, 3570−3579.
(59) Carron, K. T.; Hurley, L. G. *J. Phys. Chem.* **1991**, *95*, 9979−9984.
(60) Dhirani, A.-A.; Zehner, R. W.; Hsung, R. P.; Guyot-Sionnest, P.; Sita, L. R. *J. Am. Chem. Soc.* **1996**, *118*, 3319−3320.
(61) Zhong, C.-J.; Brush, R. C.; Anderegg, J.; Porter, M. D. *Langmuir* **1999**, *15*, 518−525.
(62) Frey, S.; Stadler, V.; Heister, K.; Eck, W.; Zharnikov, M.; Grunze, M.; Zeysing, B.; Terfort, A. *Langmuir* **2001**, *17*, 2408−2415.
(63) Nielsen, J. U.; Esplandiu, M. J.; Kolb, D. M. *Langmuir* **2001**, *17*, 3454−3459.
(64) Whelan, C. M.; Barnes, C. J.; Walker, C. G. H.; Brown, N. M. D. *Surf. Sci.* **1999**, *425*, 195−211.
(65) Sturrock, E. J.; Chen, Q.; Borchardt, P. H.; Richardson, N. V. *J. Electron Spectrosc. Relat. Phenom.* **2004**, *135*, 127−134.
(66) Duan, L.; Garrett, S. J. *J. Phys. Chem. B* **2001**, *105*, 9812−9816.
(67) Rico, M.; Barrachina, M.; Orza, J. M. *J. Mol. Spectrosc.* **1967**, *24*, 133−148.
(68) Yan, F. Q.; Qiao, M. H.; Wei, X. M.; Liu, Q. P.; Deng, J. F.; Xu, G. Q. *J. Chem. Phys.* **1999**, *111*, 8068−8076.
(69) Varsanyi, G. *Assignments for Vibrational Spectra of Seven Hundred Benzene Derivatives*; Wiley: New York, 1974.
(70) Joo, S. W.; Chung, T. D.; Jang, W.; Gong, M.-s.; Geum, N.; Kim, K. *Langmuir* **2002**, *18*, 8813−8816.
(71) Joo, S. W.; Han, S. W.; Kim, K. *J. Phys. Chem. B* **1999**, *103*, 10831−10837.
(72) Snyder, R. G. *J. Mol. Spectrosc.* **1961**, *7*, 116−144.
(73) Porter, M. D.; Bright, T. B.; Allara, D. L.; Chidsey, C. E. D. *J. Am. Chem. Soc.* **1987**, *109*, 3559−3568.
(74) Nuzzo, R. G.; Dubois, L. H.; Allara, D. L. *J. Am. Chem. Soc.* **1990**, *112*, 558−569.
(75) Walczak, M. M.; Chung, C.; Stole, S. M.; Widrig, C. A.; Porter, M. D. *J. Am. Chem. Soc.* **1991**, *113*, 2370−2378.
(76) Laibinis, P. E.; Whitesides, G. M.; Allara, D. L.; Tao, Y.-T.; Parikh, A. N.; Nuzzo, R. G. *J. Am. Chem. Soc.* **1991**, *113*, 7152−7167.
(77) Armstrong, D. R.; Clarkson, J.; Smith, W. E. *J. Phys. Chem.* **1995**, *99*, 17825−17831.
(78) Pemble, M. In *Surface Analysis: The Principal Techniques*; Vickerman, J. C., Ed.; John Wiley & Sons: New York, 1997; pp 278−282.
(79) Greenler, R. G. *J. Chem. Phys.* **1966**, *44*, 310−315.
(80) Benitez, G.; Vericat, C.; Tanco, S.; Lenicov, F. R.; Castez, M. F.; Vela, M. E.; Salvarezza, R. C. *Langmuir* **2004**, *20*, 5030−5037.
(81) Darling, S. B.; Rosenbaum, A. W.; Wang, Y.; Sibener, S. J. *Langmuir* **2002**, *18*, 7462−7468.
(82) Noh, J.; Hara, M. *Langmuir* **2001**, *17*, 7280−7285.
(83) Poirier, G. E.; Fitts, W. P.; White, J. M. *Langmuir* **2001**, *17*, 1176−1183.
(84) Poirier, G. E. *Langmuir* **1999**, *15*, 1167−1175.
(85) Godin, M.; Williams, P. J.; Tabard-Cossa, V.; Laroche, O.; Beaulieu, L. Y.; Lennox, R. B.; Grutter, P. *Langmuir* **2004**, *20*, 7090−7096.
(86) Poirier, G. E. *Chem. Rev.* **1997**, *97*, 1117−1128.
(87) Poirier, G. E.; Pylant, E. D. *Science* **1996**, *272*, 1145−1148.
(88) Kakiuchi, T.; Sato, K.; Iida, M.; Hobara, D.; Imabayashi, S.-i.; Niki, K. *Langmuir* **2000**, *16*, 7238−7244.
(89) Collard, D. M.; Fox, M. A. *Langmuir* **1991**, *7*, 1192−1197.
(90) Chidsey, C. E. D.; Bertozzi, C. R.; Putvinski, T. M.; Mujsce, A. M. *J. Am. Chem. Soc.* **1990**, *112*, 4301−4306.